

AD-A205 915

Vibrational Relaxation and Collision-Induced Dissociation of Xenon Fluoride by Neon

Prepared by

R. L. WILKINS
Aerophysics Laboratory
Laboratory Operations
The Aerospace Corporation
El Segundo, CA 90245

1 March 1989

Prepared for

SPACE DIVISION
AIR FORCE SYSTEMS COMMAND
Los Angeles Air Force Base
P.O. Box 92960
Los Angeles, CA 90009-2960

DTIC
ELECTE
S D
C E

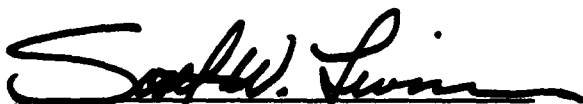
APPROVED FOR PUBLIC RELEASE;
DISTRIBUTION UNLIMITED

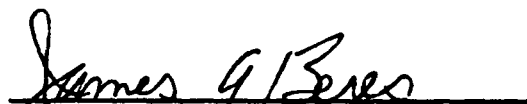
89 3 15 028

This report was submitted by The Aerospace Corporation, El Segundo, CA 90245, under Contract No. F04701-85-C-0086-P00019 with the Space Division, P.O. Box 92960, Los Angeles, CA 90009-2960. It was reviewed and approved for The Aerospace Corporation by W. P. Thompson, Director, Aerophysics Laboratory. Lt. Scott W. Levinson/CNID was the project officer.

This report has been reviewed by the Public Affairs Office (PAS) and is releasable to the National Technical Information Service (NTIS). At NTIS, it will be available to the general public, including foreign nationals.

This technical report has been reviewed and is approved for publication. Publication of this report does not constitute Air Force approval of the report's findings or conclusions. It is published only for the exchange and stimulation of ideas.


SCOTT W. LEVINSON, 1LT, USAF
Project Officer
SD/CNID


JAMES A. BERES, LT COL, USAF
Director, AFSTC West Coast Office
AFSTC/WCO OL-AB

REPORT DOCUMENTATION PAGE

1a. REPORT SECURITY CLASSIFICATION Unclassified			1b. RESTRICTIVE MARKINGS		
2a. SECURITY CLASSIFICATION AUTHORITY			3. DISTRIBUTION/AVAILABILITY OF REPORT Approved for public release; distribution unlimited.		
2b. DECLASSIFICATION/DOWNGRADING SCHEDULE					
4. PERFORMING ORGANIZATION REPORT NUMBER(S) TR-0088(3061)-1			5. MONITORING ORGANIZATION REPORT NUMBER(S) SD-TR-89-06		
6a. NAME OF PERFORMING ORGANIZATION The Aerospace Corporation Laboratory Operations		6b. OFFICE SYMBOL (If applicable)	7a. NAME OF MONITORING ORGANIZATION Space Division		
6c. ADDRESS (City, State, and ZIP Code) El Segundo, CA 90245			7b. ADDRESS (City, State, and ZIP Code) Los Angeles Air Force Base Los Angeles, CA 90009-2960		
8a. NAME OF FUNDING/SPONSORING ORGANIZATION		8b. OFFICE SYMBOL (If applicable)	9. PROCUREMENT INSTRUMENT IDENTIFICATION NUMBER F04701-85-C-0086-P00019		
8c. ADDRESS (City, State, and ZIP Code)			10. SOURCE OF FUNDING NUMBERS		
			PROGRAM ELEMENT NO.	PROJECT NO.	TASK NO.
					WORK UNIT ACCESSION NO.
11. TITLE (Include Security Classification) Vibrational Relaxation and Collision-Induced Dissociation of Xenon Fluoride by Neon					
12. PERSONAL AUTHOR(S) Wilkins, Roger L.					
13a. TYPE OF REPORT		13b. TIME COVERED FROM TO		14. DATE OF REPORT (Year, Month, Day) 1 March 1989	
				15. PAGE COUNT 25	
16. SUPPLEMENTARY NOTATION					
17. COSATI CODES			18. SUBJECT TERMS (Continue on reverse if necessary and identify by block number)		
FIELD	GROUP	SUB-GROUP	Dissociation, Vibrational Relaxation, Excimer Lasers, XeF Kinetics, Xenon Fluoride, Rate Coefficients, Neon (Mg) ⁹		
19. ABSTRACT (Continue on reverse if necessary and identify by block number)					
<p>Rate coefficients were calculated for vibrational relaxation and collision-induced dissociation of ground state xenon fluoride in neon at temperatures between 300 and 1000 K for each of nine vibrational levels. These coefficients were calculated using a pairwise additive potential energy surface, which consists of a Morse function for the XeF interaction and Lennard-Jones functions for the NeXe and NeF interactions. Rate coefficients are provided for temperature and v-dependences. The vibrational relaxation and dissociation processes occur by multiquanta transitions. Dissociation can take place from all v-levels, provided that the internal energy of the XeF molecule is close to the rotationless dissociation limit. The order of increase effectiveness of the various forms of energy in promoting dissociation in XeF was found to be translation-rotation-vibration. At room temperature, neon atoms were more efficient than helium atoms in the dissociation processes.</p>					
20. DISTRIBUTION/AVAILABILITY OF ABSTRACT <input checked="" type="checkbox"/> UNCLASSIFIED/UNLIMITED <input type="checkbox"/> SAME AS RPT. <input type="checkbox"/> DTIC USERS			21. ABSTRACT SECURITY CLASSIFICATION Unclassified		
22a. NAME OF RESPONSIBLE INDIVIDUAL			22b. TELEPHONE (Include Area Code)		22c. OFFICE SYMBOL

UNCLASSIFIED

SECURITY CLASSIFICATION OF THIS PAGE

19. ABSTRACT (Continued)

helium atoms were more efficient than neon atoms in the vibrational relaxation of XeF. Strong vibration-rotation coupling in vibrational relaxation and in the dissociation processes is demonstrated.

UNCLASSIFIED

SECURITY CLASSIFICATION OF THIS PAGE

PREFACE

The author gratefully acknowledges K. L. Foster for her invaluable assistance with the calculations and the continuing interest shown in this work by Dr. L. Wilson and the Excimer Laser Branch, Air Force Laboratory.

1. Title	✓
2. Author	✓
3. Date	✓
4. Page	✓
5. Chapter	✓
6. Section	✓
7. Subsection	✓
8. Paragraph	✓
9. Sentence	✓
10. Word	✓
11. Letter	✓
12. Digit	✓
13. Symbol	✓
14. Figure	✓
15. Table	✓
16. Equation	✓
17. Diagram	✓
18. Photograph	✓
19. Drawing	✓
20. Map	✓
21. Chart	✓
22. Graph	✓
23. Table	✓
24. Figure	✓
25. Diagram	✓
26. Photograph	✓
27. Drawing	✓
28. Map	✓
29. Chart	✓
30. Graph	✓
31. Table	✓
32. Figure	✓
33. Diagram	✓
34. Photograph	✓
35. Drawing	✓
36. Map	✓
37. Chart	✓
38. Graph	✓
39. Table	✓
40. Figure	✓
41. Diagram	✓
42. Photograph	✓
43. Drawing	✓
44. Map	✓
45. Chart	✓
46. Graph	✓
47. Table	✓
48. Figure	✓
49. Diagram	✓
50. Photograph	✓
51. Drawing	✓
52. Map	✓
53. Chart	✓
54. Graph	✓
55. Table	✓
56. Figure	✓
57. Diagram	✓
58. Photograph	✓
59. Drawing	✓
60. Map	✓
61. Chart	✓
62. Graph	✓
63. Table	✓
64. Figure	✓
65. Diagram	✓
66. Photograph	✓
67. Drawing	✓
68. Map	✓
69. Chart	✓
70. Graph	✓
71. Table	✓
72. Figure	✓
73. Diagram	✓
74. Photograph	✓
75. Drawing	✓
76. Map	✓
77. Chart	✓
78. Graph	✓
79. Table	✓
80. Figure	✓
81. Diagram	✓
82. Photograph	✓
83. Drawing	✓
84. Map	✓
85. Chart	✓
86. Graph	✓
87. Table	✓
88. Figure	✓
89. Diagram	✓
90. Photograph	✓
91. Drawing	✓
92. Map	✓
93. Chart	✓
94. Graph	✓
95. Table	✓
96. Figure	✓
97. Diagram	✓
98. Photograph	✓
99. Drawing	✓
100. Map	✓
101. Chart	✓
102. Graph	✓
103. Table	✓
104. Figure	✓
105. Diagram	✓
106. Photograph	✓
107. Drawing	✓
108. Map	✓
109. Chart	✓
110. Graph	✓
111. Table	✓
112. Figure	✓
113. Diagram	✓
114. Photograph	✓
115. Drawing	✓
116. Map	✓
117. Chart	✓
118. Graph	✓
119. Table	✓
120. Figure	✓
121. Diagram	✓
122. Photograph	✓
123. Drawing	✓
124. Map	✓
125. Chart	✓
126. Graph	✓
127. Table	✓
128. Figure	✓
129. Diagram	✓
130. Photograph	✓
131. Drawing	✓
132. Map	✓
133. Chart	✓
134. Graph	✓
135. Table	✓
136. Figure	✓
137. Diagram	✓
138. Photograph	✓
139. Drawing	✓
140. Map	✓
141. Chart	✓
142. Graph	✓
143. Table	✓
144. Figure	✓
145. Diagram	✓
146. Photograph	✓
147. Drawing	✓
148. Map	✓
149. Chart	✓
150. Graph	✓
151. Table	✓
152. Figure	✓
153. Diagram	✓
154. Photograph	✓
155. Drawing	✓
156. Map	✓
157. Chart	✓
158. Graph	✓
159. Table	✓
160. Figure	✓
161. Diagram	✓
162. Photograph	✓
163. Drawing	✓
164. Map	✓
165. Chart	✓
166. Graph	✓
167. Table	✓
168. Figure	✓
169. Diagram	✓
170. Photograph	✓
171. Drawing	✓
172. Map	✓
173. Chart	✓
174. Graph	✓
175. Table	✓
176. Figure	✓
177. Diagram	✓
178. Photograph	✓
179. Drawing	✓
180. Map	✓
181. Chart	✓
182. Graph	✓
183. Table	✓
184. Figure	✓
185. Diagram	✓
186. Photograph	✓
187. Drawing	✓
188. Map	✓
189. Chart	✓
190. Graph	✓
191. Table	✓
192. Figure	✓
193. Diagram	✓
194. Photograph	✓
195. Drawing	✓
196. Map	✓
197. Chart	✓
198. Graph	✓
199. Table	✓
200. Figure	✓
201. Diagram	✓
202. Photograph	✓
203. Drawing	✓
204. Map	✓
205. Chart	✓
206. Graph	✓
207. Table	✓
208. Figure	✓
209. Diagram	✓
210. Photograph	✓
211. Drawing	✓
212. Map	✓
213. Chart	✓
214. Graph	✓
215. Table	✓
216. Figure	✓
217. Diagram	✓
218. Photograph	✓
219. Drawing	✓
220. Map	✓
221. Chart	✓
222. Graph	✓
223. Table	✓
224. Figure	✓
225. Diagram	✓
226. Photograph	✓
227. Drawing	✓
228. Map	✓
229. Chart	✓
230. Graph	✓
231. Table	✓
232. Figure	✓
233. Diagram	✓
234. Photograph	✓
235. Drawing	✓
236. Map	✓
237. Chart	✓
238. Graph	✓
239. Table	✓
240. Figure	✓
241. Diagram	✓
242. Photograph	✓
243. Drawing	✓
244. Map	✓
245. Chart	✓
246. Graph	✓
247. Table	✓
248. Figure	✓
249. Diagram	✓
250. Photograph	✓
251. Drawing	✓
252. Map	✓
253. Chart	✓
254. Graph	✓
255. Table	✓
256. Figure	✓
257. Diagram	✓
258. Photograph	✓
259. Drawing	✓
260. Map	✓
261. Chart	✓
262. Graph	✓
263. Table	✓
264. Figure	✓
265. Diagram	✓
266. Photograph	✓
267. Drawing	✓
268. Map	✓
269. Chart	✓
270. Graph	✓
271. Table	✓
272. Figure	✓
273. Diagram	✓
274. Photograph	✓
275. Drawing	✓
276. Map	✓
277. Chart	✓
278. Graph	✓
279. Table	✓
280. Figure	✓
281. Diagram	✓
282. Photograph	✓
283. Drawing	✓
284. Map	✓
285. Chart	✓
286. Graph	✓
287. Table	✓
288. Figure	✓
289. Diagram	✓
290. Photograph	✓
291. Drawing	✓
292. Map	✓
293. Chart	✓
294. Graph	✓
295. Table	✓
296. Figure	✓
297. Diagram	✓
298. Photograph	✓
299. Drawing	✓
300. Map	✓
301. Chart	✓
302. Graph	✓
303. Table	✓
304. Figure	✓
305. Diagram	✓
306. Photograph	✓
307. Drawing	✓
308. Map	✓
309. Chart	✓
310. Graph	✓
311. Table	✓
312. Figure	✓
313. Diagram	✓
314. Photograph	✓
315. Drawing	✓
316. Map	✓
317. Chart	✓
318. Graph	✓
319. Table	✓
320. Figure	✓
321. Diagram	✓
322. Photograph	✓
323. Drawing	✓
324. Map	✓
325. Chart	✓
326. Graph	✓
327. Table	✓
328. Figure	✓
329. Diagram	✓
330. Photograph	✓
331. Drawing	✓
332. Map	✓
333. Chart	✓
334. Graph	✓
335. Table	✓
336. Figure	✓
337. Diagram	✓
338. Photograph	✓
339. Drawing	✓
340. Map	✓
341. Chart	✓
342. Graph	✓
343. Table	✓
344. Figure	✓
345. Diagram	✓
346. Photograph	✓
347. Drawing	✓
348. Map	✓
349. Chart	✓
350. Graph	✓
351. Table	✓
352. Figure	✓
353. Diagram	✓
354. Photograph	✓
355. Drawing	✓
356. Map	✓
357. Chart	✓
358. Graph	✓
359. Table	✓
360. Figure	✓
361. Diagram	✓
362. Photograph	✓
363. Drawing	✓
364. Map	✓
365. Chart	✓
366. Graph	✓
367. Table	✓
368. Figure	✓
369. Diagram	✓
370. Photograph	✓
371. Drawing	✓
372. Map	✓
373. Chart	✓
374. Graph	✓
375. Table	✓
376. Figure	✓
377. Diagram	✓
378. Photograph	✓
379. Drawing	✓
380. Map	✓
381. Chart	✓
382. Graph	✓
383. Table	✓
384. Figure	✓
385. Diagram	✓
386. Photograph	✓
387. Drawing	✓
388. Map	✓
389. Chart	✓
390. Graph	✓
391. Table	✓
392. Figure	✓
393. Diagram	✓
394. Photograph	✓
395. Drawing	✓
396. Map	✓
397. Chart	✓
398. Graph	✓
399. Table	✓
400. Figure	✓
401. Diagram	✓
402. Photograph	✓
403. Drawing	✓
404. Map	✓
405. Chart	✓
406. Graph	✓
407. Table	✓
408. Figure	✓
409. Diagram	✓
410. Photograph	✓
411. Drawing	✓
412. Map	✓
413. Chart	✓
414. Graph	✓
415. Table	✓
416. Figure	✓
417. Diagram	✓
418. Photograph	✓
419. Drawing	✓
420. Map	✓
421. Chart	✓
422. Graph	✓
423. Table	✓
424. Figure	✓
425. Diagram	✓
426. Photograph	✓
427. Drawing	✓
428. Map	✓
429. Chart	✓
430. Graph	✓
431. Table	✓
432. Figure	✓
433. Diagram	✓
434. Photograph	✓
435. Drawing	✓
436. Map	✓
437. Chart	✓
438. Graph	✓
439. Table	✓
440. Figure	✓
441. Diagram	✓
442. Photograph	✓
443. Drawing	✓
444. Map	✓
445. Chart	✓
446. Graph	✓
447. Table	✓
448. Figure	✓
449. Diagram	✓
450. Photograph	✓
451. Drawing	✓
452. Map	✓
453. Chart	✓
454. Graph	✓
455. Table	✓
456. Figure	✓
457. Diagram	✓
458. Photograph	✓
459. Drawing	✓
460. Map	✓
461. Chart	✓
462. Graph	✓
463. Table	✓
464. Figure	✓
465. Diagram	✓
466. Photograph	✓
467. Drawing	✓
468. Map	✓
469. Chart	✓
470. Graph	✓
471. Table	✓
472. Figure	✓
473. Diagram	✓
474. Photograph	✓
475. Drawing	✓
476. Map	✓
477. Chart	✓
478. Graph	✓
479. Table	✓
480. Figure	✓
481. Diagram	✓
482. Photograph	✓
483. Drawing	✓
484. Map	✓
485. Chart	✓
486. Graph	✓
487. Table	✓
488. Figure	✓
489. Diagram	✓
490. Photograph	✓
491. Drawing	✓
492. Map	✓
493. Chart	✓
494. Graph	✓
495. Table	✓
496. Figure	✓
497. Diagram	✓
498. Photograph	✓
499. Drawing	✓
500. Map	✓

A-1



CONTENTS

PREFACE	1
I. INTRODUCTION.....	7
II. COMPUTATIONAL PROCEDURE.....	11
III. DISCUSSION AND RESULTS.....	15
A. Collision Dynamics.....	15
B. State-Specific Rate Coefficients.....	18
IV. SUMMARY.....	25
REFERENCES.....	27

FIGURES

1.	(a) Typical Collision-Induced Dissociation of Ne + XeF(v=4, J=15) → Ne + Xe + F on a Potential Energy Surface for Collisions of XeF Molecules with Ne Atoms; (b) Typical Inelastic Collision of Ne + XeF(v=4, J=15) → Ne + XeF(v=2, J=73).....	16
2.	Temperature-Dependent Vibration Relaxation Rate Coefficients for Single Quantum Transitions for Ne + XeF(v) Collisions.....	19
3.	Temperature-Dependent Rate Coefficients for Dissociation from a Specific v-level in Ne + XeF(v) Collisions.....	23

TABLES

I.	Potential Parameters.....	12
II.	Typical Relaxation and Reaction Mechanisms for Ne + XeF(v, J) Collisions.....	17
III.	State-to-State Rate Coefficients for Vibrational Relaxation from a Specific v-level of XeF(v) by Ne.....	21
IV.	Rate Coefficients for Dissociation of a Specific v-level of XeF in Collision with Ne.....	22

I. INTRODUCTION

Dissociation rates of diatomic molecules have been calculated by several authors, who solved the master equations using either the vibrational-level model¹⁻⁸ or the rotational-level model.^{1,2,9-11} The master equations require, as input, state-to-state rate coefficients for vibrational and rotational relaxation and for dissociation from specific vibrational levels. The vibrational relaxation transition rates have been obtained from modified versions of Schwartz-Slowsky-Herzfeld (SSH) theory¹² in several studies, in which these rates were used to calculate vibrational nonequilibrium; the rotational effects were neglected. It has been shown theoretically¹³⁻¹⁸ and experimentally¹⁹⁻²¹ that SSH-like theories are unable to estimate vibrational transition rates for highly excited diatomic molecules. Other studies^{2,22-23} have used information theory²⁴ to calculate the vibrational transition rates; however, the validity of this method in highly excited states is not clear.^{16,18} The general conclusion of master equation studies^{1,9,25-27} is that the rotational energy states must be considered in order to account for vibrational relaxation as well as dissociation, within the framework of a single model. Haug and Truhlar²⁷ stated that a successful model must not assume that rotation is completely equilibrated for each v -level or that vibration is completely equilibrated for each J -level. Dove and Raynor⁴ concluded that thermal dissociation should be viewed as a vibrational-rotational ladder-climbing process.

Modeling the dissociation of diatomic molecules has been hampered by a lack of rate coefficients for dissociation out of specific vibrational states. Two models have been used extensively. One model assumes that diatomic dissociation occurs only from the bound level close to the rotationless dissociation limit,^{1,10,26,28} as in the ladder-climbing model;²⁹ the other model assumes that molecules can dissociate directly from all vibrational levels.^{7,30-32} Blais and Truhlar³³ have shown that most of the dissociation occurs from states within kT of the dissociation

limit. Burns and co-workers³⁴⁻³⁷ found, in their studies of dissociation of Br_2 and I_2 with rare gases, that most of the dissociation comes from states within a few kT of the dissociation limit. Similar results were found by Burns and co-workers³⁸⁻⁴⁰ for the reverse recombination reactions; their studies show that the primary requirement for dissociation of a diatomic molecule is high internal energy and that molecules with low vibrational energy can contribute to the dissociation process. Similar results have been reported by Dove and Raynor⁴ and Wilkins⁴¹ in their trajectory studies of dissociation of H_2 by He and XeF by He, respectively. The major role in dissociative collisions is played by dissociating molecules having total internal energy close to the dissociation limit and having substantial amounts of both rotational and vibrational energy. Although these models for dissociation differ radically, the total dissociation rate obtained from master equation solutions was often in agreement with experiments. Agreement with experiment, however, does not ensure the validity of a model. More accurate vibrational transition and dissociation rates are needed. Truhlar and co-workers⁵ solved the vibrational master equation for the H_2 -Ar system, where all of the required rate coefficients were calculated from quasiclassical trajectory calculations. The vibrational nonequilibrium dissociation rates were 30% less than the equilibrium dissociation rates. The nonequilibrium dissociation rates of Br_2 -Ar collisions were calculated by Burns and co-workers⁴²⁻⁴⁵ using the multiple-collision trajectory method,⁴² in which vibrational and rotational effects were included. The vibrational and rotational populations at steady state were not obtained in their calculations. Koshi et al.¹⁸ have employed the quasiclassical trajectory method to calculate vibrational transition rates and dissociation rates from specific vibrational levels for the Br_2 -Ar and the Br_2 -Br systems. They found that the vibrational transition rates in the highly excited vibrational states were quite different from those predicted from SSH-like theories. In a more recent article,⁸ they computed the full vibrational transition rate matrix for the preceding two systems using a moment analysis⁴⁶⁻⁴⁸ of the classical trajectory results. Vibrational

nonequilibrium distributions and the dissociation rates for the $\text{Br}_2\text{-Ar}$ and $\text{Br}_2\text{-Br}$ systems were obtained from a steady state solution of the master equation.

In a previous paper, Wilkins⁴¹ reported on quasiclassical trajectory calculations for the XeF-He system. Thermally averaged rate coefficients were calculated for vibrational and rotational transitions and dissociation out of specific vibrational states. It was found that relaxation and dissociation occur by multiquanta (v, J) transitions and that dissociation can take place from all v -levels, provided that the total internal energy of the XeF molecule is near the rotationless dissociation limit of ground state XeF . It was found that strong vibration-rotation coupling occurs in vibrational relaxation and dissociation processes. Gelb, Kapral, and Burns⁴⁹ have discussed the strong vibration-rotation coupling that occurs in dissociative collisions of highly energized diatomics.

The XeF ground state kinetics in helium and neon have been measured at room temperature by Fulghum et al.⁵⁰⁻⁵² and Gower et al.⁵³ and at temperatures between 23 and 95°C by Bott et al.⁵⁴ These experiments provide total decay rates or quenching rates and not the state-to-state rate coefficients required in the kinetic modeling of XeF laser performance. Fulghum et al.⁵² developed two models to extract state-to-state vibrational relaxation and dissociation rates from their experimental data using the information theoretic approach of Procaccia and Levine²⁴ to represent the vibrational relaxation rate coefficients.

The purpose of this research is to study both the temperature and v -dependences of the rate coefficients for the coupled vibrational relaxation and dissociation of XeF ground electronic state in the presence of neon. Attempts to model the performance of XeF excimer lasers have been hampered severely by a lack of knowledge of the vibrational transition rates and rate coefficients for dissociation from specific vibrational levels.

II. COMPUTATIONAL PROCEDURE

The quasiclassical Monte Carlo trajectory method has been described in a previous paper,⁵⁵ and only a brief description is provided in this report. The vibrational and rotational energy levels of ^{131}XeF are calculated from the spectroscopic data given by Tellinghuisen et al.,⁵⁶ and the vibration-rotation energy level diagram was presented in a previous paper.⁴¹ Calculations are carried out for nine vibrational states, $v=0$ through $v=8$, and for rotational states $J=0, 10, 20, 30, 40$, and 50 . A minimum of 400 trajectories are calculated for each (v, J) state of XeF at seven collision energies, starting from 0.5 through 6.5 kcal/mole, in intervals of 1.0 kcal/mole. The value of the maximum impact parameter is assumed to be $12.4 a_0$. A value of $18.0 a_0$ is assumed for the initial relative separation of the Ne atom and the center of mass of the XeF molecule. The actual technique for calculating the partitioning of the internal energy of the product species has been described adequately^{33,57} and will not be repeated here. The trajectory product pair is counted as dissociated if its internal energy exceeds the height of the rotational barrier or if the internuclear separation of the product pair exceeds $7.0 a_0$.

The potential employed here for Ne-XeF interaction is constructed by summing pairwise functions, a Morse function for the XeF interaction and a Lennard-Jones function for the NeXe and the NeF interactions. The values of the Morse potential parameters for XeF are taken from Tellinghuisen et al.⁵⁶ The values of the Lennard-Jones parameter for NeF interactions are taken from Thompson,⁵⁸ and the values for NeXe interactions are calculated using the theoretical data provided by Svehla.⁵⁹ The parameters for the Morse potential and the Lennard-Jones potentials are listed in Table I. These parameters for the Lennard-Jones potentials produce the potential curve for NeXe interaction that compares favorably with one reported by Schneider⁶⁰ in his study of potential curves of xenon with other rare gas atoms. Schneider used the model for the forces between closed shell atoms

TABLE I. Potential parameters.

Morse Function (XeF) ^a		
$D_e = 3.35$ kcal/mole		
$\alpha_e = 1.726$ a. u. ⁻¹		
$r_e = 4.367$ a. u.		
Lennard Jones Function ^b		
Pair	ϵ (eV)	σ (a.u.)
NeF	0.003460	5.223
NeXe	0.007097	7.174

^aReference 56.

^bReferences 58 and 59.

developed by Gordon and Kim⁶¹ to investigate the ground state potential energy curves of Xe-Xe, Xe-He, Xe-Ne, Xe-Ar, and Xe-Kr. Schneider found agreement between the experimentally determined values of the distance between the nuclei at the potential minimum and the depth of the potential well. The agreement was very good considering the simplicity of the calculations. The parameters used to construct the potential surface for Ne-XeF interaction are not chosen by matching any experimental data on XeF kinetics. The repulsive part of this potential is the most critical feature that affects the vibrational relaxation and dissociation.

III. DISCUSSION AND RESULTS

A. COLLISION DYNAMICS

Figure 1a exhibits typical collision-induced dissociation reaction between an Ne atom and an XeF molecule in the ($v=4$, $J=15$) state at a relative translational energy of 1399.35 cm^{-1} . This trajectory corresponds to a reactive collision, in which translational energy is converted into vibrational and rotational energy sufficient to completely dissociate the molecule. With this (TV + TR) mechanism for dissociation, the molecule climbs a vibration-rotation ladder.

Figure 1b exhibits the other type of collision that is observed on this surface that could lead to dissociation. This trajectory corresponds to a nonreactive inelastic collision, in which initial vibrational energy is converted into rotational energy, and initial translational energy is converted into rotational energy. With this (VR + TR) mechanism for dissociation, the XeF molecule climbs a rotational ladder. A quasibound molecule is formed, since the total internal energy of the molecule is above the rotationless dissociation energy of XeF and below the centrifugal barrier corresponding to the final J state. The molecule can dissociate by tunneling through this rotational barrier, or the molecule can dissociate without tunneling if its lifetime is short compared to the mean time between collisions. This analysis includes both the unbound states and the quasibound states as dissociative states.

Table II lists the percentage of collisions that results in vibrational relaxation and dissociation processes. The percentages for each (v , J) state were obtained from the calculations for 400 random collisions at an initial relative translational energy of 3.5 kcal/mole. There are three mechanisms for dissociation. Each mechanism involves the climbing of a vibration or rotation ladder. The (TV + RV) mechanism is one in which translational and rotational energy promote dissociation by increasing the vibrational energy of the molecule. This mechanism promotes

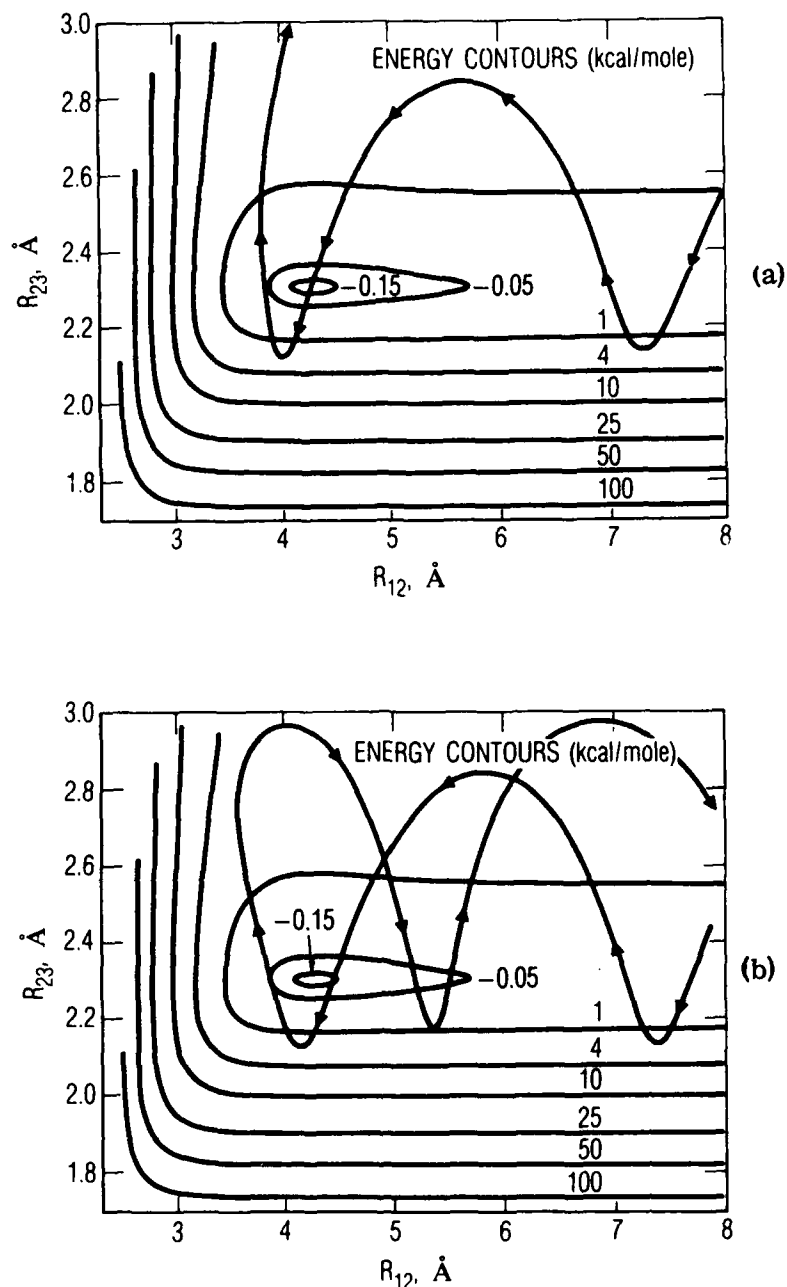


Fig. 1. (a) Typical Collision-Induced Dissociation of $\text{Ne} + \text{XeF}(v=4, J=15) \rightarrow \text{Ne} + \text{Xe} + \text{F}$ on a Potential Energy Surface for Collisions of XeF Molecules with Ne Atoms. R_{23} is the internuclear distance between Xe and F atoms; R_{12} is the internuclear distance between the Ne and Xe atoms. The energy contours are in units of kcal/mole, and the R_{12} are in units of Å. The value of the initial $E_{\text{TRANS}} = 4.0$ kcal/mole. For this system, the dissociating mechanism is (TV + TR). The XeF molecule climbs a vibration-rotation ladder. (b) Typical Inelastic Collision of $\text{Ne} + \text{XeF}(v=4, J=15) \rightarrow \text{Ne} + \text{XeF}(v=2, J=73)$. The initial $E_{\text{TRANS}} = 1.5$ kcal/mole. For this system, the dissociating mechanism is (VR + TR). The XeF molecule climbs a rotational ladder.

TABLE II. Typical relaxation and reaction mechanisms for
Ne + XeF(v, J) collisions.^a

v	J	Vibrational Relaxation			Dissociation (Reaction)		
		VR+VT	VR+TR	VT+RT	TV+RV	VR+TR	TV+TR
3	0	2.00	3.00	0.00	0.00	0.75	1.50
3	10	3.00	3.25	0.25	0.00	0.75	1.50
3	20	3.00	3.25	0.25	0.00	1.00	1.75
3	30	1.75	3.25	0.50	0.00	2.25	1.00
3	40	2.25	2.75	2.50	0.00	3.00	1.75
3	50	3.00	1.50	4.00	0.75	6.50	4.00
5	0	4.75	1.75	0.00	0.00	3.00	1.75
5	10	2.25	1.50	0.75	0.00	2.75	3.00
5	20	4.75	4.00	1.75	0.25	3.00	3.00
5	30	2.75	3.75	2.00	0.75	7.50	2.50
8	0	4.25	7.25	0.00	0.00	7.75	5.50
8	10	3.75	7.75	2.50	1.25	7.25	6.50
8	20	3.25	10.50	0.00	2.25	28.50	4.25

^aThe initial relative translational energy is 3.5 kcal/mole. Each number under a column representing a relaxation or reaction mechanism is the percent that mechanism occurs out of 400 random collisions.

dissociation by a vibrational ladder-climbing process and is not the most important mechanism for dissociating XeF. The second mechanism for dissociation, (VR + TR), is one in which one or more quanta of initial vibrational energy is converted into rotational energy, and initial translational energy is converted into rotational energy. This mechanism exhibits strong vibration-rotation coupling, and the XeF molecule climbs a rotational ladder. The third mechanism for dissociation, (TV + TR), is one in which the molecule climbs a vibration-rotation ladder. The (TV + TR) mechanism is important at low and intermediate v-levels but assumes less importance at higher v-levels with increasing J-levels. The mechanisms (VR + TR) and (TV + TR) are the key mechanisms for dissociation. In summary, dissociation occurs by vibration-rotation ladder-climbing mechanisms with strong vibration-rotation coupling.

Table II also shows the percentage of collisions that results in vibrational relaxation. The three vibrational relaxation mechanisms are (VR + TR), (VR + VT), and (VT + RT). In the (VR + TR) mechanism, the molecule climbs a rotational ladder, but the final total internal energy is below the rotationless dissociation limit. At higher v-levels, the (VR + TR) mechanism becomes the most important vibrational relaxation mechanism with increasing J-levels. The second most important mechanism for vibrational relaxation is the (VR + VT) mechanism. The third mechanism for vibrational relaxation is the (VT + RT) mechanism. This mechanism becomes more important at low v-levels with increasing J-levels and becomes less important at intermediate and high v-levels with increasing J-levels.

B. STATE-SPECIFIC RATE COEFFICIENTS

Multiquanta vibrational transitions occur in the vibrational relaxation processes. Figure 2 exhibits the temperature dependences of the state-to-state rate coefficients for vibrational relaxation processes exhibiting single-quantum vibrational transitions. At room temperature, the vibrational relaxation rates for XeF in helium⁴¹ are more efficient than in neon; for direct dissociation of XeF, the rates for neon are more rapid than those for helium. In a previous paper, Wilkins⁴¹ compared the

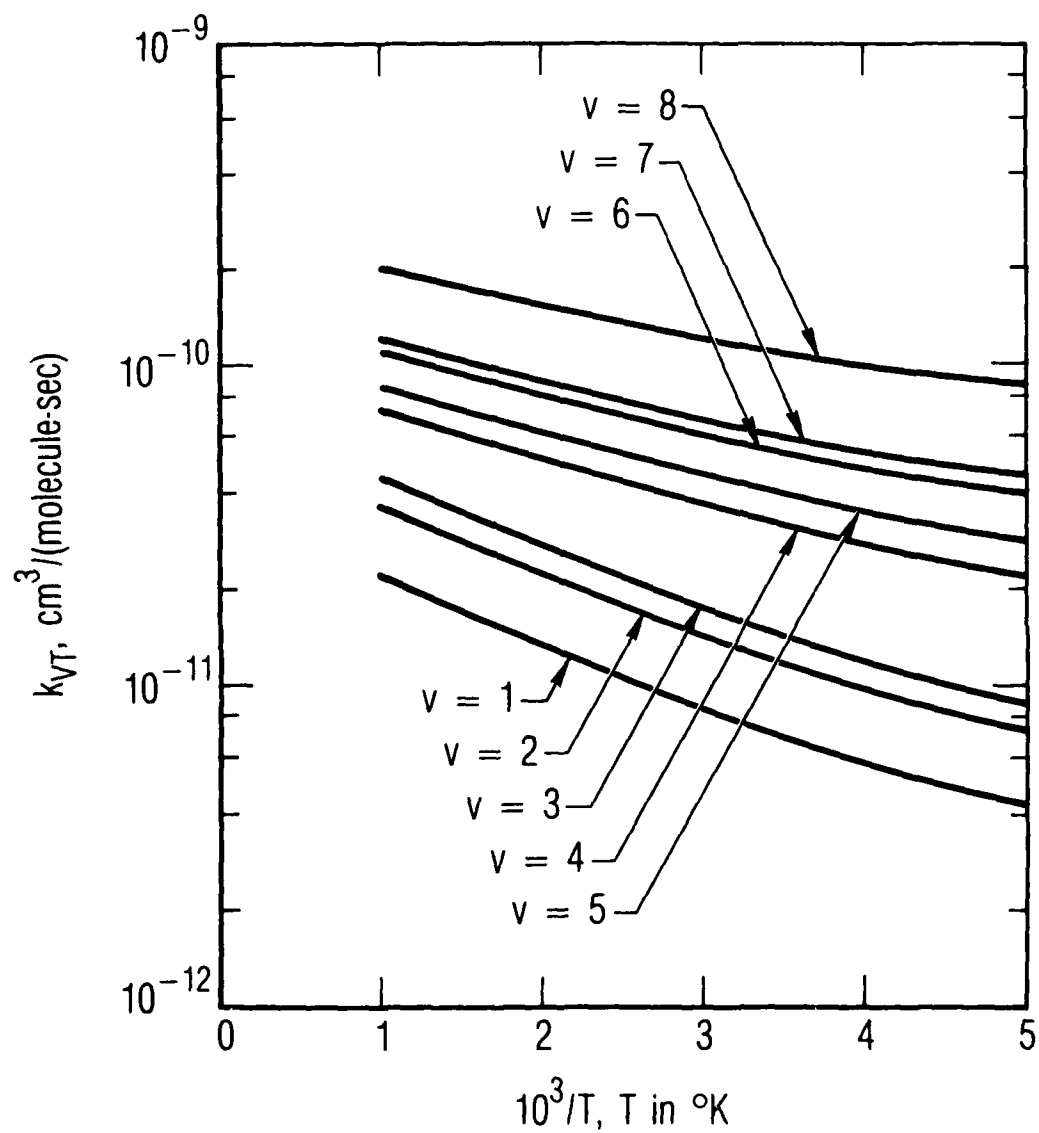


Fig. 2. Temperature-Dependent Vibration Relaxation Rate Coefficients for Single Quantum Transitions for Ne + XeF(v) Collisions

rate coefficients for these relaxation and dissociation processes of XeF in He with results obtained from a model used by Fulghum et al.⁵¹ The mass effect becomes less important with increasing temperature. Bott et al.⁵⁴ found, at room temperature, that helium and neon remove XeF population from XeF($v=1$ or $v=2$) at about the same removal rate. They found that the removal rate coefficients for argon were faster by 25%. The required temperature dependent rate coefficients for multiquanta vibrational relaxation and collision-induced dissociation from specific v -levels are listed in Tables III and IV, respectively. The vibrational relaxation rate coefficients increase with both increasing temperature and v -levels, but they do not exhibit the v^n dependence that is observed in relaxation of HF by several diluents.⁶²

Figure 3 exhibits the temperature dependences for the dissociation rate coefficients from $v=0$ to $v=8$ calculated from the trajectory study. Dissociation from $v=0$ is a very ineffective process at low temperatures but becomes more probable with increasing temperature and v -level. The molecule can dissociate from any v -level if it has total internal energy close to the dissociation limit. This can be achieved with either an initial high rotational quantum number and an initial low vibrational quantum number or vice versa.

TABLE III. State-to-state rate coefficients for vibrational relaxation from a specific v-level of XeF(v) by Ne.

$$k_{v,v'}(T) = A_{v,v'} T^n e^{-E/RT}, \text{ cm}^3/(\text{molecule}\cdot\text{sec})$$

v	v'	$-\log_{10}(A_{v,v'})$	n	E cal/mole
0	1	10.1227	-0.172	1351.0
1	0	11.0281	0.182	744.7
2	1	10.5549	0.099	807.0
2	0	9.9267	-0.239	1592.4
3	2	11.0776	0.296	615.1
3	1	10.9255	0.057	627.6
3	0	9.8873	-0.305	2396.4
4	3	9.4864	-0.155	817.4
4	2	11.1302	0.134	588.2
4	1	9.5505	-0.111	782.8
5	4	9.6450	-0.092	671.4
5	3	10.9617	0.162	667.2
5	2	11.5385	0.232	750.8
6	5	9.3325	-0.154	728.6
6	4	10.1467	-0.066	751.6
6	3	11.1833	0.163	556.1
7	6	9.7764	-0.011	529.4
7	5	10.4162	0.046	725.9
7	4	11.5195	0.258	385.3
8	7	8.9332	-0.206	665.6
8	6	9.9830	-0.037	571.2
8	5	10.0848	-0.112	614.5

TABLE IV. Rate coefficients for dissociation of a specific v-level of XeF in collision with Ne.

$$k_{\text{DISS}}(v:T) = A_v T^n e^{-E/RT}, \text{ cm}^3/(\text{molecule}\cdot\text{sec})$$

v	$-\log_{10}(A_v)$	n	E cal/mole
0	9.7931	-0.138	3798.5
1	9.1519	-0.467	2759.9
2	9.1731	-0.391	2316.2
3	10.8902	0.188	1267.2
4	10.2358	0.025	1184.3
5	10.1240	0.051	1026.4
6	9.6099	-0.041	877.0
7	10.0150	0.100	763.1
8	9.5934	0.027	358.1

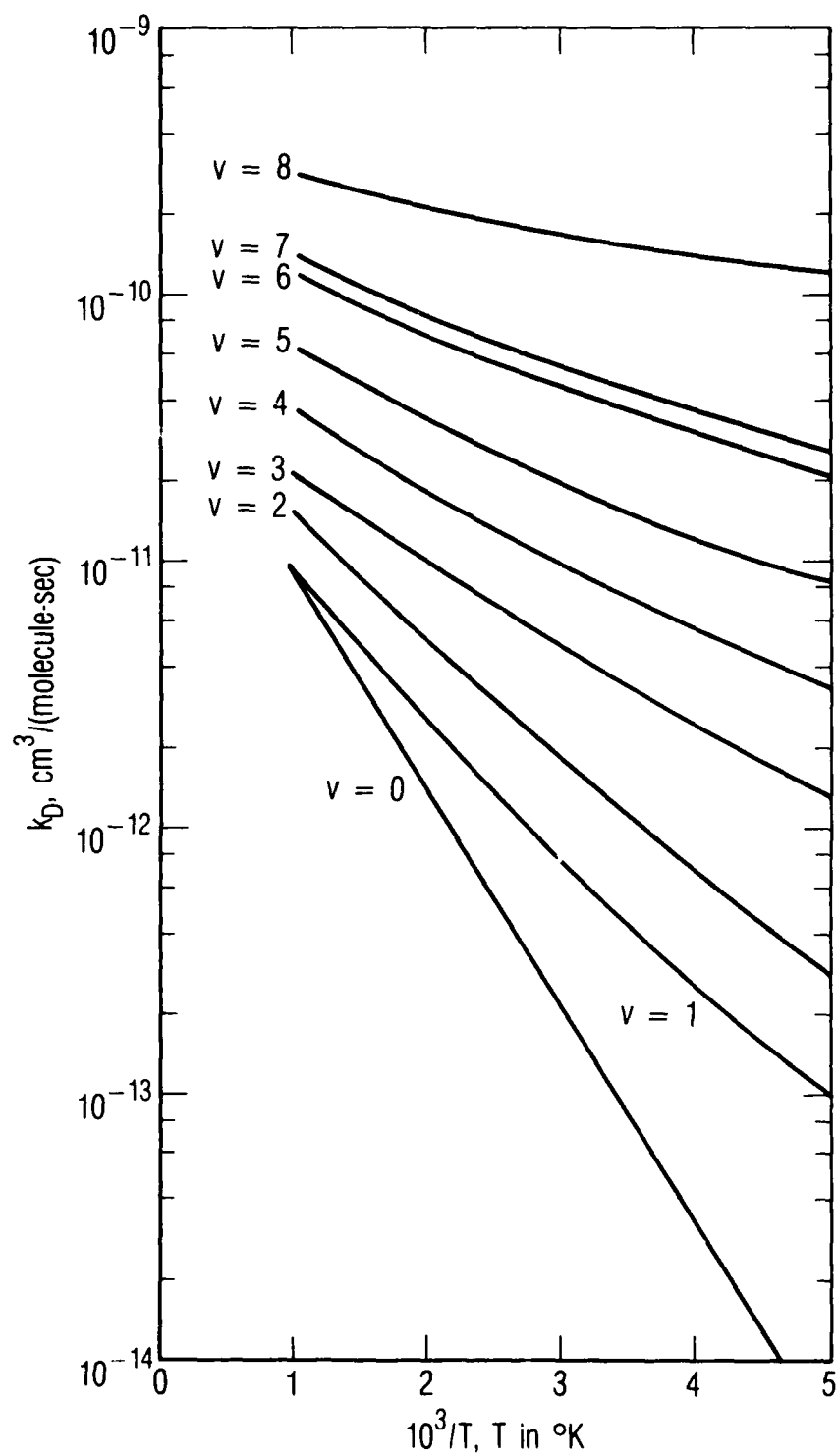


Fig. 3. Temperature-Dependent Rate Coefficients for Dissociation from a Specific v -level in $\text{Ne} + \text{XeF}(v)$ Collisions

IV. SUMMARY

A quasiclassical trajectory analysis has been used to calculate the vibrational relaxation and collision-induced dissociation rates from specific vibrational levels of XeF in collision with Ne. The state-to-state rate coefficients provided in this report can be used to study model simulations of output efficiency and multilevel laser oscillation in XeF. This study predicts a mechanism favoring dissociation from high vibrational levels but low rotational levels or from low vibrational levels with high rotational levels. The major role in dissociation is played by molecules having total internal energy close to the dissociation limit. This study predicts strong vibration-rotation coupling in both vibrational relaxation and in dissociation processes.

REFERENCES

1. H. O. Pritchard, Specialist Periodical Reports, Reaction Kinetics, Vol. 1. (The Chemical Society, London, 1975).
2. A. P. Penner and W. Forst, Chem. Phys. 11, 243 (1975).
3. S. H. Bauer, D. Hilden, and P. Jeffers, J. Phys. Chem. 80, 922 (1976).
4. J. E. Dove and S. Raynor, Chem. Phys. 28, 113 (1978); J. Phys. Chem. 83, 127 (1979).
5. D. G. Truhlar, N. C. Blais, J. C. Hayduk, and J. H. Kiefer, Chem. Phys. Lett. 63, 337 (1979).
6. J. H. Kiefer and J. C. Hajduk, Chem. Phys. 38, 328 (1979).
7. M. Ramakrisna and S. V. Babu, Chem. Phys. 42, 325 (1979); J. Chem. Phys. 68, 163 (1978); Chem. Phys. Lett. 57, 557 (1978); Chem. Phys. 36, 259 (1979).
8. H. Itoh, M. Koshi, T. Asaba, and H. Matsui, J. Chem. Phys. 82, 4911 (1983).
9. H. O. Pritchard, Acc. Chem. Res. 9, 99 (1976).
10. T. Ashton, D. L. S. Mc Elwain, and H. O. Pritchard, Can. J. Chem. 51, 237 (1973) and other papers in this series.
11. H. O. Pritchard, Can. J. Chem. 51, 3152 (1973).
12. R. N. Schwartz, Z. I. Slawsky, and K. F. Herzfeld, J. Chem. Phys. 20, 1591 (1952).
13. J. W. Duff, N. C. Blais, and D. G. Truhlar, J. Chem. Phys. 71, 4304 (1979).
14. M. Cacciatore, M. Capilelli, and G. D. Billing, Chem. Phys. 82, 1 (1983).
15. M. Robinson, B. Garetz, and J. I. Steinfeld, J. Chem. Phys. 60, 3082 (1974).
16. D. J. Nesbitt and J. T. Hynes, J. Chem. Phys. 76, 6002 (1982).
17. R. Ramaswamy and R. Bhargava, J. Chem. Phys. 80, 1095 (1984).

18. M. Koshi, H. Itoh, and H. Matsui, J. Chem. Phys. **82**, 4903 (1985).
19. G. Hancock and I. W. M. Smith, Appl. Opt. **10**, 1827 (1971).
20. L. S. Dzelskalns and F. Kaufman, J. Chem. Phys. **79**, 3836 (1983).
21. J. I. Steinfeld, Molecular Spectroscopy, edited by K. N. Rao and C. W. Mathews (Academic, New York, 1970), p. 223.
22. A. P. Penner, Mol. Phys. **36**, 1373 (1978).
23. A. J. Stace, Mol. Phys. **38**, 155 (1979).
24. I. Procaccia and R. D. Levine, J. Chem. Phys. **63**, 4261 (1975).
25. E. Kamoratos and H. O. Pritchard, Can. J. Chem. **49**, 2617 (1971).
26. J. E. Dove and D. G. Jones, Chem. Phys. Lett. **17**, 134 (1972); J. Chem. Phys. **55**, 1531 (1971).
27. K. Haug and D. G. Truhlar, J. Chem. Phys. **86**, 2697 (1987).
28. B. J. McCoy and R. G. Garborell, J. Chem. Phys. **66**, 4564 (1977); Chem. Phys. **20**, 227 (1977).
29. E. W. Montroll and K. E. Schuler, Adv. Chem. Phys. **1**, 361 (1958).
30. H. Johnston and J. Birks, Acc. Chem. Res. **5**, 327 (1972).
31. W. G. Valance, J. Phys. Chem. **85**, 1305 (1981).
32. J. H. Kiefer, H. P. G. Joosten, and W. D. Breshears, Chem. Phys. Lett. **30**, 424 (1975).
33. N. C. Blais and D. G. Truhlar, J. Chem. Phys. **70**, 2962 (1979).
34. A. G. Clarke and G. Burns, J. Chem. Phys. **58**, 1908 (1973).
35. W. H. Wong and G. Burns, Proc. R. Soc. London Ser. A **341**, 105 (1974).
36. R. K. Boyd, G. Burns, D. T. Chang, R. G. MacDonald, and W. H. Wong, Fifteenth Symposium Intl. on Combustion in Tokyo, 1974 (Combustion Institute, Pittsburgh, 1974), p. 731.
37. W. H. Wong and G. Burns, J. Chem. Phys. **62**, 1712 (1975).
38. A. G. Clarke and G. Burns, J. Chem. Phys. **55**, 4717 (1971).
39. A. G. Clarke and G. Burns, J. Chem. Phys. **56**, 4636 (1972).

40. W. H. Wong and G. Burns, J. Chem. Phys. **58**, 4459 (1973).
41. R. L. Wilkins, Theoretical Calculations of XeF Ground State Kinetics, TR-0086A(2061)-1, The Aerospace Corporation, El Segundo, Calif. (1 March 1988); J. Chem Phys. (to be published 15 November 1988).
42. D. T. Chang and G. Burns, Can. J. Chem. **55**, 380 (1977).
43. H. D. Kutz and G. Burns, Chem. Phys. **72**, 3652 (1980).
44. H. D. Kutz and G. Burns, J. Chem. Phys. **74**, 3947 (1981).
45. G. Burns and L. K. Cohen, J. Chem. Phys. **78**, 3245 (1982).
46. R. J. Gordon, J. Chem. Phys. **67**, 5923 (1977).
47. D. G. Truhlar and J. W. Duff, Chem. Phys. Lett. **36**, 551 (1975).
48. V. Halanel and R. D. Levine, Chem. Phys. Lett. **46**, 35 (1977).
49. A. Gelb, R. Kapral, and G. Burns, J. Chem. Phys. **56**, 4631 (1972).
50. S. F. Fulghum, I. P. Herman, M. S. Feld, and A. Javan, Appl. Phys. Lett. **33**, 926 (1978).
51. S. F. Fulghum, M. S. Feld, and A. Javan, Appl. Phys. Lett. **35**, 247 (1979).
52. S. F. Fulghum, M. S. Feld, and A. Javan, IEEE JQE **16**, 815 (1980).
53. M. C. Gower, R. Exberger, P. D. Rowley, and K. W. Billman, Appl. Phys. Lett. **33**, 65 (1978).
54. J. F. Bott, R. F. Heidner, J. S. Holloway, J. B. Koffend, and M. A. Kwok, Measurement of XeF Ground State Dissociation and Vibrational Equilibration, TR-0088(3930-04)-1, The Aerospace Corporation, El Segundo, Calif. (25 March 1988); J. Chem. Phys. (to be published October 1988).
55. R. L. Wilkins, J. Chem. Phys. **63**, 534 (1975).
56. P. C. Tellinghuisen and J. Tellinghuisen, Appl. Phys. Lett. **43**, 898 (1983).
57. N. C. Blais and D. G. Truhlar, J. Chem. Phys. **65**, 5335 (1976); **66**, 772 (1977); **70**, 2962 (1979).
58. D. L. Thompson, J. Chem. Phys. **78**, 1763 (1983).

59. R. A. Svehla, NASA Technical Report R-132 (1962).
60. B. Schneider, J. Chem. Phys. 58, 4447 (1973).
61. R. G. Gordon and Y. S. Kim, J. Chem. Phys. 56, 3122 (1972).
62. N. Cohen, M. A. Kwok, R. L. Wilkins, and J. F. Bott, AIAA-83-1699, AIAA 16th Fluid and Plasma Dynamics Conference, July 12-14, 1983, Danvers, Mass.

LABORATORY OPERATIONS

The Aerospace Corporation functions as an "architect-engineer" for national security projects, specializing in advanced military space systems. Providing research support, the corporation's Laboratory Operations conducts experimental and theoretical investigations that focus on the application of scientific and technical advances to such systems. Vital to the success of these investigations is the technical staff's wide-ranging expertise and its ability to stay current with new developments. This expertise is enhanced by a research program aimed at dealing with the many problems associated with rapidly evolving space systems. Contributing their capabilities to the research effort are these individual laboratories:

Aerophysics Laboratory: Launch vehicle and reentry fluid mechanics, heat transfer and flight dynamics; chemical and electric propulsion, propellant chemistry, chemical dynamics, environmental chemistry, trace detection; spacecraft structural mechanics, contamination, thermal and structural control; high temperature thermomechanics, gas kinetics and radiation; cw and pulsed chemical and excimer laser development including chemical kinetics, spectroscopy, optical resonators, beam control, atmospheric propagation, laser effects and countermeasures.

Chemistry and Physics Laboratory: Atmospheric chemical reactions, atmospheric optics, light scattering, state-specific chemical reactions and radiative signatures of missile plumes, sensor out-of-field-of-view rejection, applied laser spectroscopy, laser chemistry, laser optoelectronics, solar cell physics, battery electrochemistry, space vacuum and radiation effects on materials, lubrication and surface phenomena, thermionic emission, photo-sensitive materials and detectors, atomic frequency standards, and environmental chemistry.

Computer Science Laboratory: Program verification, program translation, performance-sensitive system design, distributed architectures for spaceborne computers, fault-tolerant computer systems, artificial intelligence, micro-electronics applications, communication protocols, and computer security.

Electronics Research Laboratory: Microelectronics, solid-state device physics, compound semiconductors, radiation hardening; electro-optics, quantum electronics, solid-state lasers, optical propagation and communications; microwave semiconductor devices, microwave/millimeter wave measurements, diagnostics and radiometry, microwave/millimeter wave thermionic devices; atomic time and frequency standards; antennas, rf systems, electromagnetic propagation phenomena, space communication systems.

Materials Sciences Laboratory: Development of new materials: metals, alloys, ceramics, polymers and their composites, and new forms of carbon; non-destructive evaluation, component failure analysis and reliability; fracture mechanics and stress corrosion; analysis and evaluation of materials at cryogenic and elevated temperatures as well as in space and enemy-induced environments.

Space Sciences Laboratory: Magnetospheric, auroral and cosmic ray physics, wave-particle interactions, magnetospheric plasma waves; atmospheric and ionospheric physics, density and composition of the upper atmosphere, remote sensing using atmospheric radiation; solar physics, infrared astronomy, infrared signature analysis; effects of solar activity, magnetic storms and nuclear explosions on the earth's atmosphere, ionosphere and magnetosphere; effects of electromagnetic and particulate radiations on space systems; space instrumentation.